Mon. Not. R. Astron. Soc. **000**, 000–000 (0000) Printed 25 November 2014 (MN LATEX style file v2.2)

The hybrid, coronal lines nova V5588 Sgr (2011 N.2) and its six repeating secondary maxima

U. Munari[1], A. Henden[2], D.P.K. Banerjee[3], N.M. Ashok[3], G.L. Righetti[4]
S. Dallaporta[4] and G. Cetrulo[4]
[1]*INAF Astronomical Observatory of Padova, 36012 Asiago (VI), Italy*
[2]*AAVSO, 49 Bay State Rd. Cambridge, MA 02138, USA*
[2]*Astronomy and Astrophysics Division, Physical Research Laboratory, Navrangapura, Ahmedabad - 380 009, Gujarat, India*
[4]*ANS Collaboration, c/o Osservatorio Astronomico, via dell'Osservatorio 8, 36012 Asiago (VI), Italy*

arXiv:1411.6297v1 [astro-ph.SR] 23 Nov 2014

25 November 2014

ABSTRACT

The outburst of Nova Sgr 2011 N.2 (=V5588 Sgr) was followed with optical and near-IR photometric and spectroscopic observations for 3.5 years, beginning shortly before the maximum. V5588 Sgr is located close to Galactic center, suffering from E_{B-V}=1.56 (±0.1) extinction. The primary maximum was reached at V=12.37 on UT 2011 April 2.5 (±0.2), and the underlying smooth decline was moderately fast with t_2^V=38 and t_3^V=77 days. On top of an otherwise normal decline, six self-similar, fast evolving and bright secondary maxima (SdM) appeared in succession. Only very few other novae have presented so clear secondary maxima. Both the primary maximum and all SdM occurred at later times with increasing wavelengths, by amounts in agreement with expectations from fireball expansions. The radiative energy released during SdM declined following an exponential pattern, while the breadth of individual SdM and the time interval between them widened. Emission lines remained sharp (FWHM∼1000 km/s) throughout the whole nova evolution, with the exception of a broad pedestal with a trapezoidal shape (Δvel=3600 km/sec at the top and 4500 km/sec at the bottom) which was only seen during the advanced decline from SdM maxima and was absent in between SdM. V5588 Sgr at maximum light displayed a typical FeII-class spectrum which did not evolve into a nebular stage. About 10 days into the decline from primary maximum, a typical high-ionization He/N-class spectrum appeared and remained visible simultaneously with the FeII-class spectrum, qualifying V5588 Sgr as a rare *hybrid* nova. While the FeII-class spectrum faded into oblivion, the He/N-class spectrum developed strong [FeX] coronal lines.

Key words: novae, cataclysmic variables

1 INTRODUCTION

V5588 Sgr was discovered at unfiltered 11.7 mag on 2011 Mar 27.832 UT as PNV J18102135−2305306 = Nova Sgr 2011 N.2 by Nishiyama and Kabashima (2011). Spectroscopic confirmation was obtained on Mar. 28.725 UT by Arai et al. (2011) who noted prominent emission lines of Hα (FWHM=900 km/s), Hβ and Fe II (multiplets 42, 48, 49) on a highly reddened continuum. Very red colors were evident in the first photometric observations obtained on Mar 28.670 UT by Kiyota (2011) and on Mar 28.788 UT by Maehara (2011), characterized by $B-V$∼1.7.

The peculiar nature of V5588 Sgr soon started to emerge when Munari et al. (2011a) reported about a bright and fast evolving secondary maximum reaching peak brightness on April 25.0 UT, and when Munari et al. (2011b) observed a further secondary maximum peaking on May 22.0 UT. Their optical and IR spectra showed emission lines having two components, whose relative intensity greatly changed at the time of the secondary maxima, one narrow with FWHM=1050 km/s and one broad with full-width-at-zero-intensity (FWZI) of 4700 km/sec. The intensity ratio between the broader and the narrow component was larger in HeI than in HI lines. Rudy et al. (2011) wrote about IR spectroscopic observations for April 28 and they too noted the two-component structure of emission lines, which was also present in the IR spectroscopic observations for April 26, 28 and May 4 described by Banerjee and Ashok (2011).

The latter also reported a weak line seen at 2.0894 microns, which was earlier tentatively identified as a coronal line due to [MnXIV] in the few instances where it has been seen in novae spectra (in nova V1974 Cyg by Wagner and Depoy 1996; in RS Oph by Banerjee et al. 2009).

Radio observations of V5588 Sgr were first carried out with E-VLA on Apr 21.5, Apr 30.3 and May 1.3 UT by Krauss et al. (2011a). These observations, soon before and after the April 25.0 UT secondary maximum, failed to detect the nova, which was instead radio-bright when observed on May 14.5 and 15.5 UT (a week before the May 22 secondary maximum) by Krauss et al. (2011b). According to Krauss et al. (2011c) the nova was again radio quiet on June 2.2, radio loud on June 15.4, and once again radio quiet on July 27.1. Krauss et al. (2011c) noted how the observed fast rises in radio emission could not be explained in the framework of a simple expanding isothermal sphere as modelled in many other novae, and that non-detections could be taken as upper limits to the thermal flux from the nova ejecta which indicate that V5588 Sgr is quite distant ($\geqslant$9 kpc) and likely associated with the Galactic central regions.

In this paper we present our photometric and spectroscopic monitoring of the evolution of V5588 Sgr, that tightly covers the first 200 days from pre-maximum to well into the advanced decline when conjunction with the Sun prevented further observations. The later decline was followed by sparser photometric observation extending up to mid 2014.

2 OBSERVATIONS

2.1 Optical photometric observations

BVR_CI_C optical photometry was obtained with (*a*) ANS Collaboration telescopes N. 30, 37, 100 and 157, and (*b*) AAVSO.net telescopes K35 and T61. The same local photometric sequence, spanning a wide color range and carefully calibrated against Landolt (2009) equatorial standards, was used at all telescopes and observing epochs, ensuing a high consistency among different data sets. The BVR_CI_C photometry of the nova is given in Table 1, where the quoted uncertainties are the total error budget, which combines the measurement error on the variable with the error associated to the transformation from the local to the standard photometric system (as defined by the photometric comparison sequence around the nova linked to the Landolt's standards).

The operation of ANS Collaboration telescopes is described in detail by Munari et al. (2012) and Munari & Moretti (2012). They are all located in Italy. The median values of the total error budget of their measurements reported in Table 1 are: $\sigma(B)$= 0.016, $\sigma(V)$= 0.009, $\sigma(R_C)$= 0.004, $\sigma(I_C)$= 0.007, $\sigma(B-V)$= 0.016, $\sigma(V-R_C)$= 0.009, and $\sigma(V-I_C)$= 0.011. All measurements on the program nova were carried out with aperture photometry, the long focal length of the telescopes and the absence of nearby contaminating stars not requiring to revert to PSF-fitting. Concerning ANS Collaboration telescopes, colors and magnitudes are obtained separately during the reduction process, and are not derived one from the other.

Both AAVSO.net telescopes K35 and T61 are robotically operated from AAVSO Headquarters in Cambridge

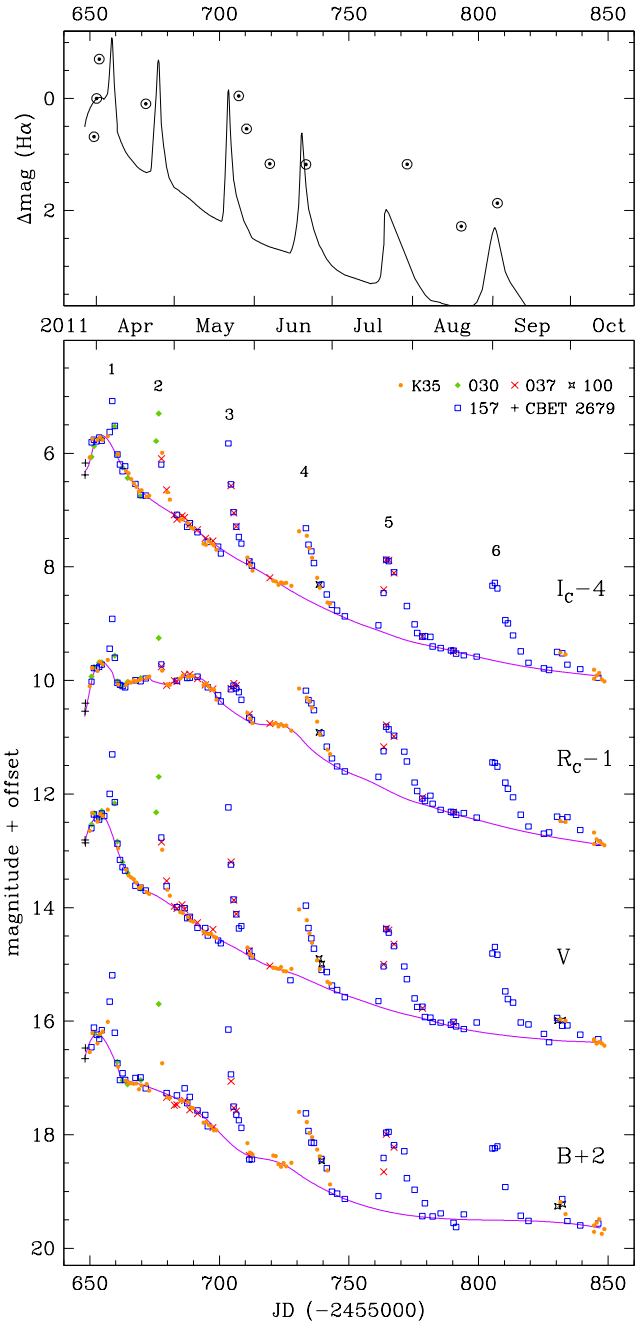

Figure 1. *Lower panel:* BVR_CI_C photometric evolution of V5588 Sgr during 2011 (the different telescopes are identified in the legend at upper right). The solid lines are hand-drawn to guide the eye in following the normal nova decline away from secondary maxima. The largely different shape of the R_C lightcurve is due to the extremely strong Hα emission line that largely dominated the flux recorded through the band-pass. *Upper panel:* evolution of the Hα emission line integrated flux. The ordinate scale is the same of the lower panel and the zero point is set to 1.080×10^{-10} erg cm^{-2} sec^{-1} corresponding to the flux for day −0.4 spectrum (2011 Apr 02; cf Table 2), the one closest to photometric maximum. For comparison, the interpolated V-band lightcurve from the lower panel is superimposed.

Table 1. BVR_CI_C photometry of V5588 Sgr (the long table is published in its entirety in the electronic edition of this journal. A portion is shown here for guidance regarding its form and content).

date	*tel.*	*HJD*	B	$\pm$	V	$\pm$	R_C	$\pm$	I_C	$\pm$	$B-V$	$\pm$	$V-R_C$	$\pm$	$V-I_C$	$\pm$	R_C-I_C	$\pm$
Mar 30.164	157	650.664	14.461	0.005	12.601	0.003	11.051	0.004	9.805	0.014	1.855	0.004	1.557	0.002	2.796	0.012	1.253	0.011
Mar 31.131	157	651.631	14.115	0.024	12.358	0.004	10.814	0.004	9.762	0.008	1.821	0.017	1.564	0.001	2.596	0.006	1.084	0.006
Mar 31.149	030	651.649	14.211	0.014	12.341	0.006	10.761	0.006	9.872	0.009	1.829	0.014	1.633	0.008	2.557	0.013	0.996	0.010
Apr 01.142	157	652.642	14.237	0.011	12.430	0.005	10.814	0.004	9.789	0.008	1.885	0.007	1.698	0.003	2.661	0.006	1.092	0.005
Apr 02.129	157	653.629	14.314	0.012	12.452	0.003	10.788	0.003	9.720	0.006	1.872	0.007	1.681	0.002	2.752	0.005	1.109	0.005
Apr 02.150	030	653.650	14.261	0.016	12.431	0.008	10.680	0.009	9.750	0.007	1.872	0.015	1.704	0.008	2.727	0.007	1.071	0.009
Apr 03.123	157	654.623	14.159	0.006	12.342	0.004	10.752	0.002	9.778	0.005	1.800	0.003	1.625	0.005	2.612	0.008	1.033	0.003

Table 2. Log of the optical spectroscopic observations.

date UT (2011)	HJD	Δt (days)	expt. (sec)	resol. power	disp (Å/pix)	range (Å)	telesc.
Mar 31.123	651.623	−2.4	600		2.31	3200−7950	1.22m+B&C
Apr 01.134	652.634	−1.4	1200		2.13	3950−8640	0.61m+MMS mk.II
Apr 02.147	653.647	−0.4	1200		2.31	3200−7950	1.22m+B&C
Apr 10.125	661.625	+7.6	1800	10,000		6400−6800	0.61m+MMS mk.II
Apr 20.122	671.622	+17.6	2400		2.31	3300−7900	1.22m+B&C
May 19.072	700.572	+46.6	1200	17,000		4800−7350	1.82m+Echelle
May 25.969	707.469	+53.5	3600		1.17	5300−7300	0.70m+MMS mk.I
May 28.983	710.483	+56.5	9000		1.17	4500−7500	0.70m+MMS mk.I
Jun 06.953	719.453	+65.5	9000		1.17	4500−7500	0.70m+MMS mk.I
Jun 20.922	733.422	+79.4	9000		1.17	4500−7500	0.70m+MMS mk.I
Jul 29.951	772.451	+118	7200		2.31	3500−7650	1.22m+B&C
Aug 19.846	793.346	+139	3600		2.31	3600−7740	1.22m+B&C
Sep 02.799	807.299	+153	3600		2.31	3600−7740	1.22m+B&C
Sep 03.804	808.304	+154	1800		0.21	6300−6700	0.70m+MMS mk.I

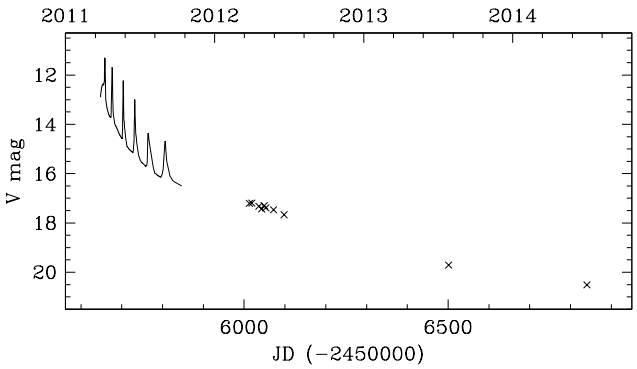

Figure 2. V-band evolution of V5588 Sgr during the advanced decline. The interpolated V-band lightcurve from Figure 1 is superimposed for comparison.

(MA, USA). K35 (located in Weed NM, USA) was used during the initial monitoring of the nova up to the end of June 2011, when the arrival of the monsoon season prevented further observations, which briefly resumed in October 2011 before the solar conjunction. T61 (located at Mt. John, New Zealand) was used at later epochs, when longer integrations were necessary to catch the ever fainter nova. The data reduction of AAVSO.net data provides V and colors, obtained via aperture photometry for K35 observations, and PSF fitting for T61.

2.2 Optical spectroscopy

Optical spectroscopy of V5588 Sgr has been obtained with three telescopes. A log of the observations is given in Table 2.

ANS Collaboration 0.70m telescope located in Polse di

Table 3. Near-IR photometry of V5588 Sgr.

Date (2011)	JD - 2455000	J	H	K
Apr 26	678.387	8.19 ± 0.04	7.59 ± 0.05	6.75 ± 0.04
May 04	686.473	8.90 ± 0.02	8.73 ± 0.03	7.88 ± 0.09
May 07	689.442	9.01 ± 0.03	8.92 ± 0.04	7.97 ± 0.12
May 08	690.412	9.06 ± 0.03	8.99 ± 0.03	8.11 ± 0.15
May 18	700.457	9.58 ± 0.02	9.39 ± 0.05	8.59 ± 0.12
May 23	705.385	9.04 ± 0.02	8.69 ± 0.02	7.95 ± 0.07
May 26	708.453	9.40 ± 0.03	9.18 ± 0.05	8.23 ± 0.12
June 11	724.280	10.06 ± 0.04	9.90 ± 0.05	-

Cougnes (Udine, Italy) and operated by GAPC Foundation is equipped with a mark.I Multi Mode Spectrograph, and obtained medium-resolution spectra with a front illuminated Apogee ALTA U9000 CCD camera (3056×3056 array, 12μm pixel, KAF9000 sensor). ANS Collaboration 0.61m telescope operated by Schiaparelli Observatory in Varese and equipped with a mark.II Multi Mode Spectrograph obtained low-resolution and Echelle spectra with a SBIG ST10XME CCD camera (2192×1472 array, 6.8 μm pixel, KAF-3200ME chip with micro-lenses to boost the quantum efficiency). The optical and mechanical design, operation and performances of Multi Mode Spectrographs from Astrolight Instruments in use within ANS Collaboration are described by Munari and Valisa (2014).

Low resolution spectroscopy of V5588 Sgr was obtained also with the 1.22m telescope + B&C spectrograph operated in Asiago by the Department of Physics and Astronomy of the University of Padova. The CCD camera is a ANDOR iDus DU440A with a back-illuminated E2V 42-10 sensor, 2048×512 array of 13.5 μm pixels. It is highly efficient in the blue down to the atmospheric cut-off around 3200 Å, and it is normally not used long ward of 8000 Å for the fringing affecting the sensor.

The spectroscopic observations at all three telescopes were obtained in long-slit mode, with the slit rotated to the parallactic angle. All observations have been flux calibrated, and the same spectrophotometric standards have been adopted at all telescopes. All data have been similarly reduced within IRAF, carefully involving all steps connected with correction for bias, dark and flat, sky subtraction, wavelength and flux calibration.

2.3 Near-infrared observations

The near-IR photometric and spectroscopic observations of V5588 Sgr were carried out from 1.2m Mt. Abu tele-

Table 4. Log of the near-IR spectroscopic observations.

Date (2011)	JD (-2455000)	Δt (days)	Exp. time (sec) J	H	K
Apr 26	678.463	+24.5	200	200	200
May 04	686.440	+32.4	120	120	120
May 05	687.441	+33.4	120	120	120
May 06	688.458	+34.5	120	150	160
May 18	700.406	+46.4	120	150	160
May 23	705.319	+51.3	150	150	150
May 24	706.365	+52.4	150	150	150
May 25	707.361	+53.4	150	150	150
May 26	708.340	+54.3	120	180	180

scope, operated by Physical Research Laboratory (India). The JHK spectra were obtained at similar dispersions of $\sim$ 9.5 Angstrom/pixel in each of the J, H, K bands using the Near-Infrared Imager/Spectrometer which uses a 256 X 256 HgCdTe NICMOS3 array. A set of two spectra were taken with the object dithered to two positions along the slit which were subtracted from each other to eliminate the sky contribution and the detector dark counts. The spectra were then extracted using IRAF and wavelength calibration was done using a combination of OH sky lines and telluric lines that register with the stellar spectra. Following the standard procedure, the object spectra were then ratioed with the spectra of a comparison star (SAO 186061; spectral type B9V) observed at similar airmass as the object and from whose spectra the Hydrogen Paschen and Brackett absorption lines had been extrapolated out. The ratioed spectra were then multiplied by a blackbody curve at the effective temperature of the comparison star to yield the final spectra. Photometry in the JHK bands was done in photometric sky conditions using the imaging mode of the NICMOS3 array. Several frames, in five dithered positions offset typically by 20 arcsec, were obtained of both the nova and a selected standard star in each of the J, H, K filters. Near-IR JHK magnitudes were then derived using IRAF tasks and following the regular procedure followed by us for photometric reduction (e.g. Banerjee & Ashok 2002, Naik et al. 2010). The log of the near-IR photometric and spectroscopic observations are given in Tables 3 and 4.

3 PHOTOMETRIC EVOLUTION

The photometric evolution of V5588 Sgr in the BVR_CI_C bands during 2011 is presented in Figure 1. The 2012-2014 portion of the lightcurve is displayed in Figure 2, while the evolution in the near-IR JHK bands is displayed in Figure 3. Figure 4 identifies the remnant in the surrounding crowded field and Figure 5 provides a zoomed view onto the secondary maxima and the color evolution.

The photometric evolution of V5588 Sgr is unlike that of other novae: on top of otherwise smooth and normal-looking maximum and decline phases, six bright secondary maxima appeared. These secondary maxima were fast evolving and followed a clear pattern: their duration and the time interval between them were increasing with successive maxima.

Secondary maxima appearing on top the lightcurve of otherwise smoothly evolving novae (thus not to be confused

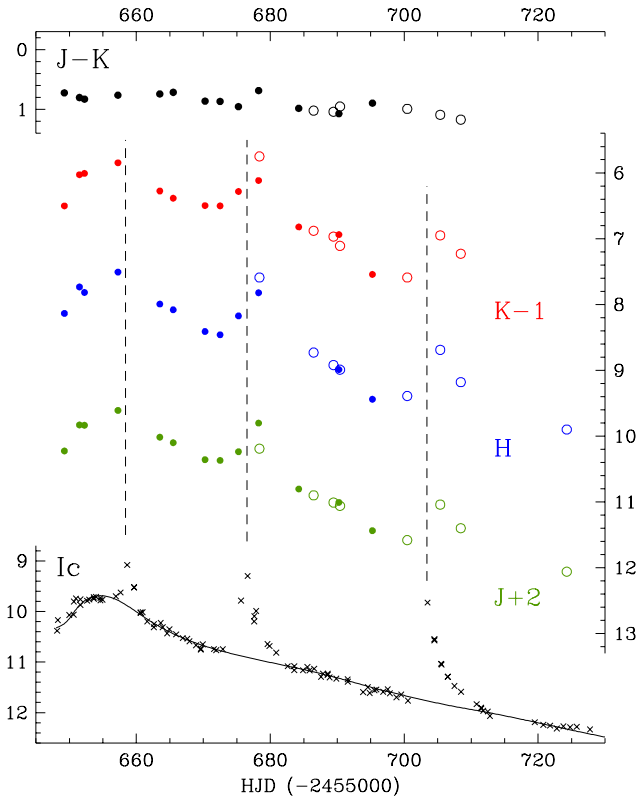

Figure 3. Near-IR JHK photometric evolution of V5588 Sgr. Open circles: our data from Table 3. Dots: data from Kanata Observatory 1.5m telescope. The I_C lightcurve is reproduced from Figure 1 for comparison with optical data.

with the rebrightenings that some slow novae display around maximum, like V723 Cas or V1548 Aql, or around the transition from optically thick to optically thin conditions, like V1494 Aql or V2468 Cyg) are quite rare. Some novae (eg. Nova Aql 1994a, Nova Cyg 2006, Nova Cyg 2008b; Venturini et al. 2004, Munari et al. 2008a, Munari et al. 2011c), have displayed just one such event over their recorded photometric history. Strope et al. (2010) in their review of AAVSO lightcurves of a hundred novae, termed J-type (from "jitter") the novae showing multiple secondary maxima. Among the lightcurves of J-type novae they presented, the one closer to V5588 Sgr is - by far - Nova Sgr 2003 (=V4745 Sgr), that displayed five bright secondary maxima but had a completely different spectroscopic evolution (see below).

We first discuss the underlying smooth photometric evolution of V5588 Sgr as if belonging to an otherwise normal nova, and then turn our attention to the secondary maxima.

3.1 Optical

The underlying smooth photometric evolution of V5588 Sgr is highlighted in Figures 1 and 5 by the continuous lines drawn from simple cubic spline interpolations. The time ($\pm$0.2 days) and brightness of the *normal* maximum (as opposed to the subsequent six secondary maxima, labelled 1 to 6 in Figure 1) as determined from these interpolations are:

$$t^B_{max} = 2455653.5 \quad B_{max} = 14.178 \qquad (1)$$

t^V_{max} = 2455654.0 V_{max} = 12.368
t^{Rc}_{max} = 2455654.3 Rc_{max} = 10.654
t^{Ic}_{max} = 2455654.7 Ic_{max} = 9.689

The epoch of maximum occurred at later times for longer wavelength bands, the maximum in I_C coming ∼1.2 days after that in the B band. This delay is similar to the 1.0 days observed in Nova Aql 2009 (V1722 Aql) by Munari et al. (2010) who noted how it closely followed the expectations for the initial fireball expansion phase. At maximum the nova appeared faint and highly reddened, which contributed to limited interest among observers and inhibited monitoring programs for e.g. in the X rays or UV. A wider interest arose only after the first secondary maxima were reported, but at that time the nova had already dropped in brightness.

The times (in days) taken by V5588 Sgr to decline by 2 and 3 magnitudes in the B and V bands are

$$t^B_2 = 50 \qquad t^B_3 = 90 \qquad (2)$$
$$t^V_2 = 38 \qquad t^V_3 = 77$$

They are in the normal proportion among themselves (cf Munari et al. 2008a, Eq. 2).

An interesting feature of the early photometric evolution is the single pulsation-like oscillation that occurred right before maximum (highlighted in Figure 5). The single cycle had an amplitude of about ∼0.2 mag and was completed in ∼4 days. A similar feature was observed also in V2615 Oph (Nova 2007) at the time of maximum brightness, with the cycle having an amplitude of ∼1.5 mag and being completed in ∼8 days (Munari et al. 2008b). In both novae the $B−V$ color did not change much in phase with the observed cycle, while $V−I_C$ varied in a way reminiscent of pulsation (bluer at maximum, redder at minimum). Such a feature could be related to the pre-maximum halts observed in some novae (e.g. Hounsell et al. 2010). Theoretical investigations are beginning to explore in some greater detail the early lightcurve of novae, and short-lived features similar to the pulsation-like oscillation we observed in V5588 Sgr are emerging in the computations, as in those of Hillman et al. (2014).

The R_C-band lightcurve of V5588 Sgr in Figure 1 looks quite different from that in the other bands. This is due to the presence of an extremely strong Hα in emission. While other remission lines counted for a minimal fraction of the flux recorded over the B, V, and I_C bands, the Hα dominated the flux recorded through the R_C band, from 30% on our first spectrum (day −2.4) to 79% on the last (Sep 2).

The near-IR photometric evolution of V5588 Sgr is presented in Figure 3 where our data from Table 3 is supplemented with public data from Kanata Observatory 1.5m telescope[1]. In the near-IR V5588 Sgr behaved similarly to the optical: a smooth underlying decline on which are superimposed the secondary maxima. Over the limited period of time covered by Figure 3, the $J−K$ color slowly and smoothly increased by only a small amount, indicating that no warm dust condensed in the ejecta. The secondary maxima were not accompanied by significant $J−K$ color changes. Even if the time of primary maximum is not well covered by JHK data, nonetheless Figure 3 suggests that in the near-IR it occurred later than in the optical, in accordance with expectations from an expanding fireball (e.g. Seaquist & Bode 2008). An important feature displayed by Figure 3 is how the secondary maxima occurred about two days later in JHK than at optical wavelengths. Such a shift and its amount suggest that broad-band emission during SdM were dominated by expanding photospheres.

[1] http://kanatatmp.g.hatena.ne.jp/kanataobslog/20110514

3.2 Reddening and distance

van den Bergh and Younger (1987) derived a mean intrinsic color $(B-V)_\circ$=+0.23 ±0.06 for novae at maximum, and $(B-V)_\circ$=−0.02 ±0.04 for novae at t_2. The photometric evolution in Figure 1 and the data in Table 1 show that V5588 Sgr was measured at $(B-V)$=+1.81 at maximum, and $(B-V)$=+1.52 at t_2. The corresponding reddenings are E_{B-V}=1.58 and 1.54, for a mean value E_{B-V}=1.56 (±0.1), which will be adopted in the rest of this paper. The corresponding extinction would be A_V=5.16 mag following the reddening relations calibrated by Fiorucci and Munari (2003). The high reddening affecting V5588 Sgr is confirmed by the OI emission line ratio in the infrared observations of Rudy et al. (2011), and by the flux ratio of Paschen to Brackett emission lines in our near-IR spectra.

Both the rate of decline and the observed magnitude 15 days past maximum are popular methods of estimating the distance to a nova.

The relation $M_{\max} = \alpha_n \log t_n + \beta_n$ as most recently calibrated by Downes & Duerbeck (2000) provides a distance to V5588 Sgr of 7.8 kpc for t^V_2, and 7.5 kpc for t^V_3. The specific stretched S-shaped curve first suggested in analytic form by Capaccioli et al. (1989) gives a distance of 7.1 kpc in the revised form proposed by Downes & Duerbeck (2000). Buscombe & de Vaucouleurs (1955) suggested that all novae have the same absolute magnitude 15 d after maximum light. Its most recent calibration by Downes & Duerbeck (2000) returns 8.1 kpc as the distance to V5588 Sgr. The straight average of these four determinations is an absolute magnitude M_V=−7.2 and a distance of 7.6 kpc, that we will adopt in this paper.

Such a large distance is consistent with the upper limit of negative radio detections discussed by Krauss et al. (2011c). Considering the galactic coordinates of the nova l=7.84 and b=−1.88, it seems likely that V5588 Sgr is associated with the Galactic center and the inner Bulge.

3.3 Astrometric position and progenitor/remnant

We have derived an accurate astrometric position for V5588 Sgr on K35 images (3.5m focal length) around maximum brightness. The average position from 8 R_C images obtained between 2011-03-30 and 2011-04-02 is (equinox 2000):

$$\alpha = 18^h\ 10^m\ 21^s.339 \qquad \delta = -23^\circ\ 05'\ 30''.09 \qquad (3)$$

with an uncertainty of 40 milli-arcsec on both. Figure 4 provides a deep finding chart for the remnant.

At the nova position there is no counterpart on the Palomar I and II plates or 2MASS and WISE catalogs. At the reddening and distance of V5588 Sgr, a M2-3 III cool giant similar to those present in novae RS Oph and T CrB would shine at K∼11.8, a sub-giant of the type present in nova U

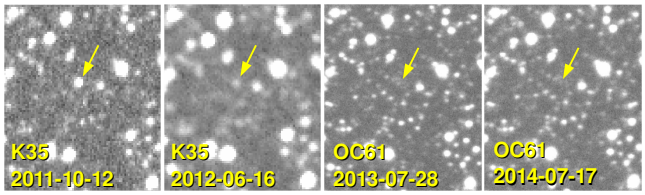

Figure 4. Sequence of V-band images (1.7 arcmin on the long side, North to the top, East to the left) of the advanced decline of V5588 Sgr to pin-point the position of the nova and aid with the identification of the progenitor and/or relic. The nova is seen at $V\sim$20.5 on the 2013-07-28 image and it is fainter than 21.0 mag in the 2014-07-17 image.

Sco at $K\sim$15.2, and an M0 main sequence star at $K\sim$20.3. Considering that the 2MASS survey did not detect stars fainter than 13.5 mag in K within 2 arcmin of the position of the nova, we may only exclude a cool giant as the donor star in V5588 Sgr, while a sub-giant and a main sequence donor star are equally allowed by the 2MASS limiting magnitude. Similar conclusions can be reached considering the $V\sim$21.1 upper limit to the nova renmant brightness from our latest observation on July 17, 2014.

4 MULTIPLE SECONDARY MAXIMA

The most striking feature displayed by V5588 Sgr is undoubtedly the six secondary maxima (SdM for short) that adorn the lightcurve in Figure 1, with Figure 5 providing a zooming on them all. Their basic properties are summarized in Table 5.

The SdM look similar, although not identical. The time interval between them increased along the series, with an interval of 18 days between the first two and twice as much (42 days) between the last two. Similarly, the duration of SdM also increased along the series, from FWHM=2.1 days for the first to FWHM=8.6 days for the last. The photometric colors at peak SdM brightness changed along the six episodes. Compared to the underlying normal decline, the first three SdM were redder by 0.5 mag in $B-V$ and bluer by the same mount in $V-I_{\rm C}$, indicating that the energy distribution of the continuum source associated to the SdM was sharply peaking at V-band wavelengths. The color change associated with the fourth SdM was similarly directed but of lower amplitude, while the last two SdM were not accompanied by significant color changes. In the near-IR, a minimal blueing in $J-K$ color was observed during the second SdM, while the third saw no changes at all (cf. Figure 3).

The first two SdM were brighter than the primary maximum of the nova in all $BVR_{\rm C}I_{\rm C}$ bands, and the third equal in $BVI_{\rm C}$ bands. As mentioned above, the $\sim$2 days time delay between peak brightness at optical and near-IR wavelengths (cf. Figure 3) suggests that broad-band emission during an SdM was governed by photospheric expansion as in a fireball. The projected areas of the expanding fireballs associated with the first two SdM were therefore larger than the one for the primary maximum. The very rapid evolution of SdM in comparison with the underlying normal nova evolution, suggests that a much lower amount of material was ejected at a much larger velocity than at primary maximum. The fact that the emission during SdM was primarily continuum radiation is confirmed by Figure 1, where the $R_{\rm C}$ lightcurve shows much less pronounced SdM and the Hα flux evolution does not follow the SdM pattern.

Table 5. Basic parameters for the secondary maxima (SdM). The heliocentric JD is HDJ + 2455000; Δt is the time elapsed between successive SdM; FWHM measures the width in time of SdM; peak V mag is listed next; ΔV is the amplitude of SdM measured from the extrapolated underlying normal nova decline (cf. Figure 2); M_V is the absolute magnitude reached by the SdM after removing the contribution by the extrapolated underlying normal nova decline; Flux$_{bol}^{BVRI}$ is expressed in units of 10^{-4} erg cm^{-2} and represent the sum over the optical bands of the net flux recorded during the SdM (i.e. net the extra flux superimposed to the underlying smooth nova decline), corrected for E_{B-V}=1.56 reddening and a standard R_V=3.1 reddening law.

sec.max. N.	1	2	3	4	5	6
HJD$_{\rm max}$	658.5	676.5	703.5	731.8:	764.4	806.2
UT (2011)	Apr	Apr	May	Jun	Jul	Sep
	7.0	25.0	22.0	19.3:	21.9	1.7
Δt (days)		18	27	28	33	42
FWHM (days)	2.1	2.0	3.8	7.6	8.4	8.6
V peak	11.30	11.70	12.23	13.00:	14.37	14.70
ΔV	1.39	2.12	2.41	2.13:	1.42	1.54
M_V	−7.89	−7.69	−7.21	−6.42:	−4.85	−4.56
Flux$_{bol}^{BVRI}$	21.2	13.6	8.9	6.7:	5.0	3.4

We have built SdM profiles for $BR_{\rm C}I_{\rm C}$ similar to those presented in Figure 5 for the V band, and we have integrated their net flux (i.e. the energy radiated in *excess* of the underlying normal nova lightcurve). The sum of the energy radiated during SdM in the four optical bands is listed in the last raw of Table 5 and plotted in Figure 6, where a nice exponential decline is evident.

5 SPECTROSCOPIC EVOLUTION

The spectral evolution at optical wavelengths is presented in Figure 7, and that in the near-IR in Figures 9, 10 and 11, while Figure 8 highlights the evolution of the profile of hydrogen emission lines.

5.1 An hybrid nova

At the time of discovery, the first confirmatory spectroscopic observation by Arai et al. (2011, on day −4.78) describes the spectrum of V5588 Sgr as that of a typical FeII-type nova (Williams 1992) with prominent emission lines of Hα (FWHM=900 km/s), Hβ and Fe II (multiplets 42, 48, 49) on a highly reddened continuum. Our early optical spectra in Figure 7 (epochs −2.4 and −0.4 days) confirm the FeII classification, and the high resolution Hα profile for day +7.6 in Figure 8 shows a strong P-Cyg absorption component (blue-shifted by 650 km/s with respect to the emission component; FWHM(em)=770 km/s, FWHM(abs)=200 km/s) which is typical of FeII novae around maximum light (e.g. McLaughlin 1960).

Our next spectrum in Figure 7, obtained on day +18, just before the rise to second SdM, shows something quite unexpected: in addition to the initial FeII-type spectrum,

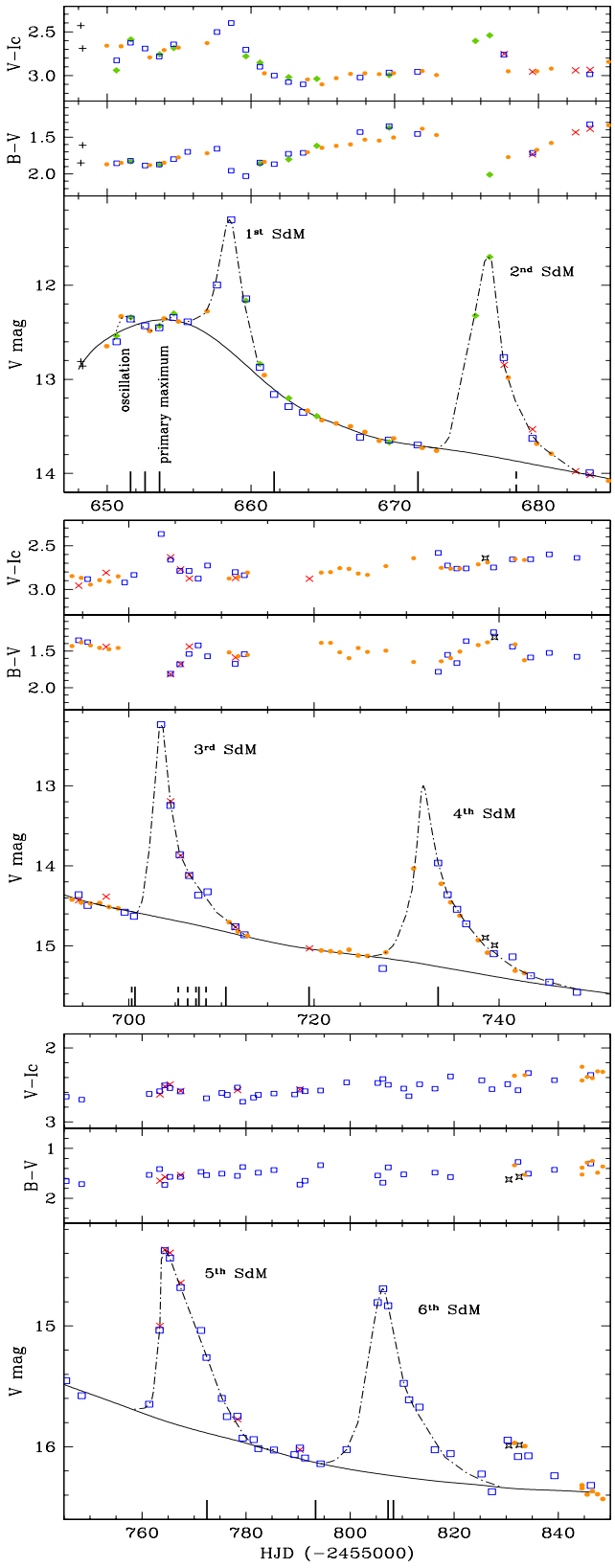

Figure 5. Expanded view of the six secondary minima (SdM), highlighted by the hand drawn dot-dashed lines. The solid line represents the underlying normal nova evolution. The symbols for the different telescopes are identified in Figure 1. Solid and dashed vertical bars mark the epochs of optical and near-IR spectroscopic observations, respectively.

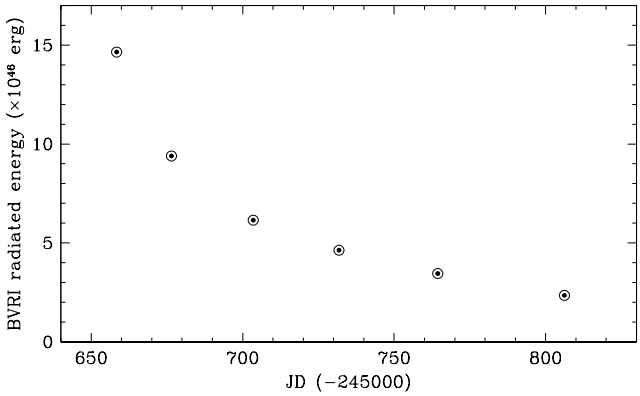

Figure 6. Net energy radiated through BVR_CI_C bands by the six secondary maxima (for a distance to V5588 Sgr of 7.6 kpc, and corrected for E_{B-V}=1.56 and R_V=3.1 extinction).

there is now simultaneously present the spectrum of a fully flagged He/N-type nova, with a stunning diplay of HeI and HeII lines. On subsequent epochs the FeII-type spectrum declined in strength, without developing the nebular lines (most notably [OIII]) that usually dominates the advanced decline of FeII-type novae. This agrees with the fact that the lightcurves in Figure 1 do not show the typical flattening of the brightness decline. In FeII-type novae, the transition from optically thick (emitting mostly permitted lines) to optically thin ejecta (dominated by nebular lines) occurs between 3 and 4 mag below maximum, when the photometric decline all of a sudden changes from rapid to a much flatter one (McLaughlin 1960, Munari 2012). While during the optically thick decline the gas in the ejecta is just mainly recombining, during the optically thin phase the hard radiation field from the central WD permeates the ejecta with a strong re-ionization action. There is available on the web[2], a spectrum for April 12 obtained with the Kanata 1.5m telescope that shows how He/N-type spectrum was already emerging at that time (day +10), when V5588 Sgr had just ended the first SdM and was back to the smooth underlying decline (see Figure 5). We may therefore conclude that the appearance of the He/N-type spectrum coincided with the nova entering the evolutionary phase characterized by the SdM. The last of our spectra still showing (feeble) traces of the FeII-type spectrum is that for day +118, after that date the recorded spectrum is only that of a He/N nova.

There are only very few novae that have been seen to evolve from a FeII- to an He/N-type spectrum or to have simultaneously shown them both. Williams (1992) called them *hybrid* novae and reviewed their basic characteristics. He observed how they (*a*) display unusually broad FeII lines, and (*b*) tend to evolve like normal He/N novae once the transition from the initial FeII- to the final He/N-type has been completed. V5588 Sgr distinguish itself from the other hybrid novae on both these points.

First of all V5588 Sgr displayed *narrow* emission lines during the FeII phase, certainly not larger than seen in normal FeII novae. As shown in Figures 7 and 8, the FWHM of Balmer and FeII emission lines kept lower than 1000 km/s throughout the whole FeII phase. In hybrid novae, the

[2] http://kanatatmp.g.hatena.ne.jp/kanataobslog/20110416/p1

FWHM of emission lines during the FeII phase is at least twice as large as seen in V5588 Sgr, and remain similarly broad during the subsequent He/N phase. Secondly, V5588 Sgr evolved slowly for a He/N. The t_3 characteristic times of He/N novae are short, from a few days to a maximum of a few weeks, while for V5588 Sgr it was a few months (2.5 months in V and 3 in B band, see Eq.(2) above). In addition, the width at half maximum of emission lines in He/N novae is usually equal or larger than 2500 km/sec, and their profile is more fat-topped than Gaussian-like. In V5588 Sgr the HeI and HeII lines are stable at FWHM∼1100 km/sec through out the recorded evolution, with a profile well fitted by a Gaussian, marginally double-peaked with a velocity separation of ∼400 km/sec. Finally during the advanced decline of He/N novae, the intensity of HeII emission line is usually larger than Hβ. In V5588 Sgr, HeII never grew in intensity to more than half of Hβ.

The hybrid classification from optical spectra is not in contrast with available observations in the near-IR. Our first JHK spectra were obtained on day +24.5 (when optical spectra were already dominated by He/N features and the signatures from the FeII phase were weakening), and their appearance is typical of He/N novae, as are all the other near-IR spectra we obtained (Figures 9, 10 and 11). On the other hand, Rudy et al. (2011) labelled their near-IR spectrum of V5588 Sgr for day +25.5 as that of a FeII nova, without the carbon lines. The absence of carbon lines is obvious in our spectra. As shown in Banerjee and Ashok (2012), the FeII class of novae early after outburst, are distinguished from the He/N class by displaying a large number of strong carbon lines in each of the J,H and K bands. Most prominent among these CI lines are the 1.165, 1.175 μm region features in the J band and the strong cluster of lines beyond Br10 in the H band in the 1.74 to 1.80 μm region. Examples of these CI lines can be seen in the spectra of several FeII type novae viz., V1280 Sco and V2615 Oph (Das et al. 2008; Das, Banerjee & Ashok 2009), V2274 Cyg (Rudy et al. 2003), V1419 Aql (Lynch et al. 1995) and V5579 Sgr (Raj, Ashok & Banerjee 2011). Earlier near-IR spectra, obtained around primary maximum, would have been highly valuable to check if the FeII type characterizing optical wavelengths at that time was similarly dominating the near-IR.

5.2 Coronal lines

As noted by Williams (1992), the advanced evolution of He/N-type novae proceeds in one of three distinct ways: (*a*) permitted emission lines simply fade away and nebular emission lines are not observed, (*b*) strong [NeIII] 3869, 3868 Å o [NeV] 3346, 3426 Å lines emerge, resulting in a *neon* nova, or (*c*) coronal forbidden lines such as [FeX] 6375 Å develop.

V5588 Sgr did not show usual nebular lines. It also did not develop [NeV], and only feeble traces of [NeIII] and [NeIV] were visible, therefore it did not turn into a neon nova. It instead developed prominent [FeX], stronger than [FeVII] 6087 Å at peak intensity on day +139 spectrum in Figure 7, fully qualifying V5588 Sgr as a *coronal line* nova. [ArX] 5534 Å was probably present too, and [FeXI] 3987 could marginally be so. [ArXI] 6019, [NiXV] 6702, [NiXIII] 5115 Å which were prominent in nova RS Oph (Wallerstein & Garnavich 1986, Iijima 2009) were not present, while not much can be said for [FeXIV] 5303 Å given the presence of nearby and strong [CaV] 5309 Å.

[FeX] became visible for the first time on our spectrum for day +18, shortly before the onset of the second SdM, simultaneous with the first appearance of HeII in emission, signalling the ejecta were turning optically transparent and nuclear burning was proceeding in the WD envelope. Under such conditions, novae are usually detected as strong super-soft X-ray sources (Krautter 2008). Unfortunately, the Swift satellite did not observe V5588 Sgr until much later. The intensity of [FeX] increased with time and in pace with HeII (cd Figure 7), peaking in intensity on our spectrum for day +139 (2011 Aug 19), obtained during the normal decline between fifth and sixth SdM. Quite interestingly, on our last spectrum, obtained two weeks later (day +153) and right at the peak of sixth secondary maximum, both HeII and [FeX] are instead missing. We see two alternative explanation for this: either (*a*) the nuclear burning on the surface of the WD stopped sometime between day +139 and +153 and the consequent rapid cooling brought the temperature of the WD below the threshold for producing HeII and [FeX], or (*b*) the material ejected during the sixth SdM temporarily obscured the view of the WD and inner regions of the ejecta, where the HeII and [FeX] form, or from where it was coming the hard radiation capable of forming them in the external ejecta. The time scale for recombination in the ejecta goes as:

$$t_{\rm rec} \approx 0.66 \left(\frac{T_{\rm e}}{10^4\ {\rm K}}\right)^{0.8} \left(\frac{n_{\rm e}}{10^9\ {\rm cm}^{-3}}\right)^{-1} {\rm (hours)} \qquad (4)$$

following Ferland (2003). At the critical density for [FeX] (log$N_{\rm crit}$=9.7 cm^{-3}), the recombination time scale is very short, less than one hour for any reasonable choice of the electronic temperature $T_{\rm e}$. Of course, after the switch-off of the nuclear burning, the envelope of the WD is still very hot and cools off gradually, so the input of high energy photons to the ejecta is not instantaneously stopped. Nonetheless, there seem to be enough time between the spectra of +139 and +153 to allow enough cooling of the WD to stop producing [FeX] lines from regions with an electron density close to the critical value.

However, [FeVII] 6087 Å too disappeared from day +153 spectrum. This line came from regions characterized by an electron density lower that its critical value (log$N_{\rm crit}$=7.6 cm^{-3}) but higher than that of absent [OIII] lines (log$N_{\rm crit}$=5.8 cm^{-3}), so with a recombination time from a few hours up to a couple of months. The disappearance of [FeVII] 6087 Å line could therefore pose a problem for alternative "a" above. An even more serious problem comes from the text of an approved Target of Opportunity proposal (available on the web) for Swift X-ray observations of V5588 Sgr to be carried out in 2012 that states the nova was displaying at the time of proposal submission (2012 May 18, or day +411) a [FeX] emission line half the intensity of [FeVII] on optical spectra, and thus observations were requested to observe the expected super-soft X-ray emission.

We are tempted to conclude that [FeX] was still visible long after the end of our optical spectroscopic monitoring, and that the absence of [FeX] and HeII from the day +153 spectrum at the peak of the sixth SdM was caused by optically thick material ejected during such SdM blocking the view toward inner ejecta and central star. Unfortunately, for

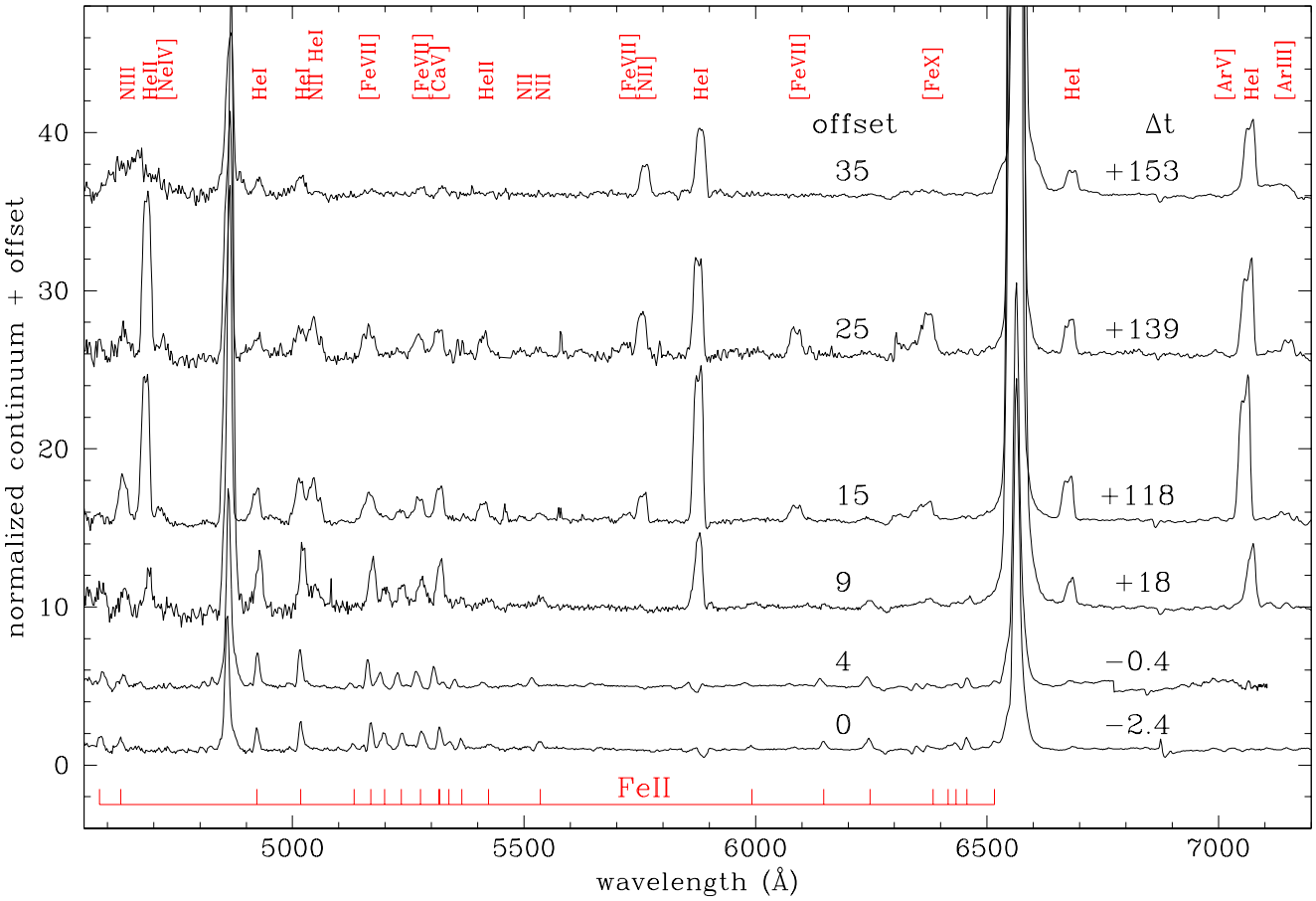

Figure 7. Evolution of optical spectra, clearly showing the hybrid nature of V5588 Sgr.

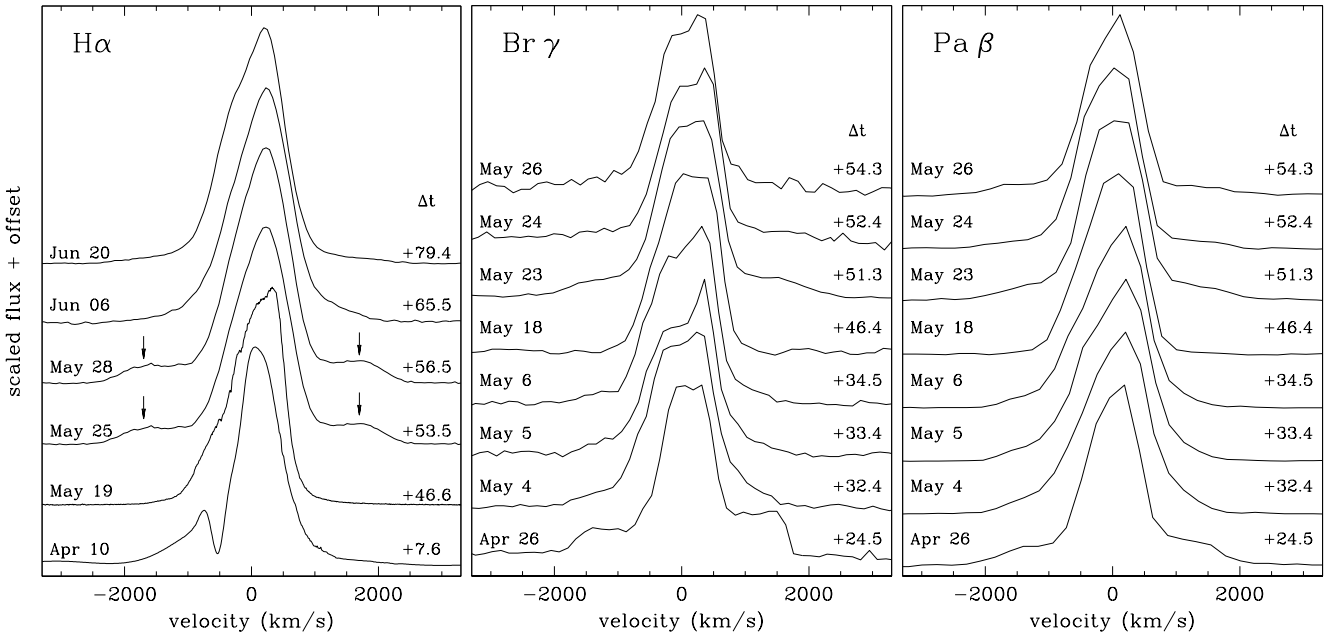

Figure 8. Profiles at different epochs of hydrogen Hα, Brγ and Paα emission line profiles. The arrows on the left panel highlight the presence of the broad pedestal appearing at selected dates.

none of the other SdM there are optical spectra obtained during the rise in brightness or around maximum to check if this was a repeating pattern through all observed SdM.

5.3 The variable two-components line profiles

The emission lines of V5588 Sgr displayed throughout the whole recorded outburst show a narrow profile, with FWHM∼1000 km/sec for both optical and near-IR spectra. However, sometimes a much broader and weak pedestal appeared at the bottom of the narrow and much stronger component. This is well seen in Figure 8, where the broad pedestal in obvious in the Hα profiles for days +53.5 and +56.5, or the Brγ and Paβ profiles for days +24.5 and +51.3. On the Hα profiles of Figure 8, the pedestal has a trapezoidal shape, extending for Δvel=3600 km/sec at the top and 4500 km/sec at the bottom. The shape is similar for Brγ and Paβ, with reduced velocities: 2900 at the top and 3600 at the bottom. The limited resolution of our spectra does not allow to distinguish between a boxy, flat-topped profile and two separate emission symmetric with respect to the main component, in other words if the emission from the pedestal originates in a filled prolate volume or in a bipolar arrangement.

A most important fact to note is that, both at optical and near-IR wavelengths, the broad pedestal to Hydrogen lines is not seen in between SdM, or during their rising toward maximum and early decline from it, but only during the advanced decline from SdM maximum and before the return to the smooth decline between SdM. The broad component developed similarly for HeI lines, as Figure 11 well illustrates from K-band spectra: on Apr 26 and May 23, when the pedestal was present in Brγ, it was so also for HeI 2.0581 μm, while on other dates only the narrow component was visible in HeI as for Brγ. The pedestal to HeI is prominent in near-IR spectra, while it is too faint to be seen in optical spectra.

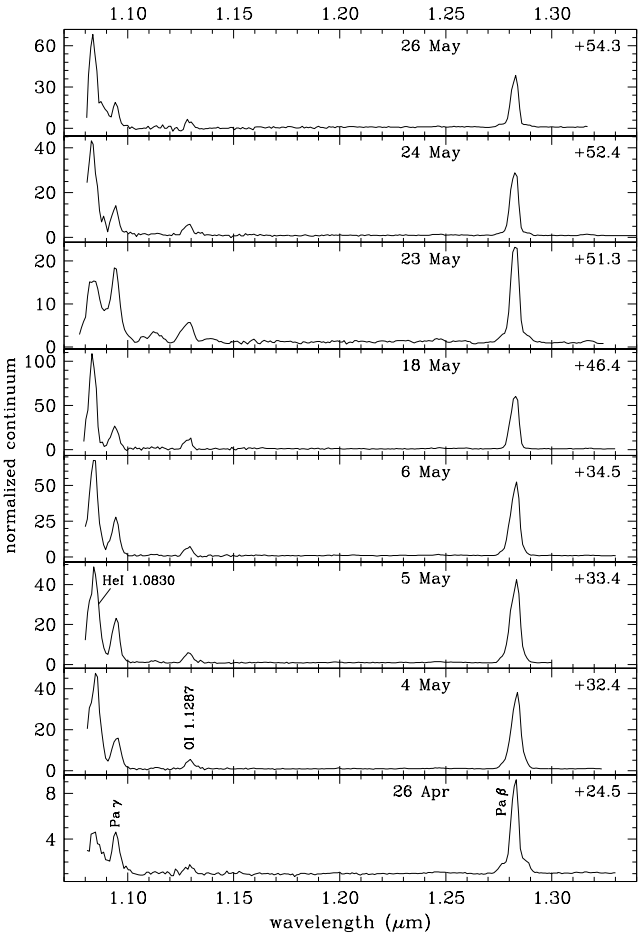

Figure 9. J band spectra of V5588 Sgr with prominent lines marked. Weak lines of OI 1.3164 μm and NI 1.2461,69 μm are also detected which can be seen if the spectra are magnified. All spectra are normalized to unity at 1.25 μm at which the corresponding observed fluxes are (in chronological order) 11.8, 8.7, 8.44, 8.13, 4.64, 7.62, 6.83, 6.11 and 5.47×10^{-17} W/cm^2/μm.

5.4 A few NIR lines worth a special mention

While most of the HI, HeI and OI lines in Figures 9, 10 and 11 are routinely seen in the NIR spectra of novae (Banerjee and Ashok, 2012), there are a few features which need special mention. These are the features at 1.6872 and 1.7414 μm in the H band and a K band feature at $\sim$ 2.089 μm. Both the H band features are clearly seen in Figure 3 and although their origin is not certain, they could possibly be due to Fe II. The 1.6872 μm line is seen to slowly gain in strength to equal and even surpass the adjacent Br11 line. In the near-infrared, there are a few FeII lines seen in the spectra of novae, which are believed to be primarily excited by Lyman α and Lyman continuum fluorescence. Among these are the so-called "one micron Fe II lines" seen at around the 1 micron region in several novae (Rudy et al. 2000 and references therein). In addition, two other Fe II lines at 1.6872 and 1.7414 μm in the H band, have also proposed to be pumped by the same mechanism (Banerjee, Das & Ashok 2009; Bautista et al. 2004). The H band lines are prominently detected in the 2006 outburst of recurrent nova RS Oph (Banerjee, Das & Ashok 2009), in the slow nova V2540 Oph (Rudy et al 2002a), in V574 Pup (Naik et al. 2010) and possibly also in the recurrent nova CI Aql (Lynch et al. 2004). As the detections of these lines in individual objects increase, it becomes amply evident that these H band lines could be present in the spectra of other novae too, but have evaded detection because of blending - especially when their widths are large - with the Br 11 (1.6806 μm) line.

An emission feature at ∼2.090 μm in the K band is also seen in the spectra at most of the epochs of observation. Two possible identifications may be considered for this line. First, it could be FeII 2.0888 μm, a line also seen in the nova V2615 Oph (Das, Banerjee & Ashok 2009)for which an excitation mechanism by Lyman α fluorescence was proposed. Alternatively, this feature could be the [Mn XIV] 2.0894 μm coronal line which has been seen in a few instances in novae spectra during the coronal phase viz., in nova V1974 Cyg (Wagner & Depoy, 1996) and in RS Oph (Banerjee, Das & Ashok 2009). It should be noted that the ∼2.090 μm line should not be confused with an unidentified line at 2.0996 μm that has often been detected in novae and which still remains unidentified (Rudy et al. 2002b).

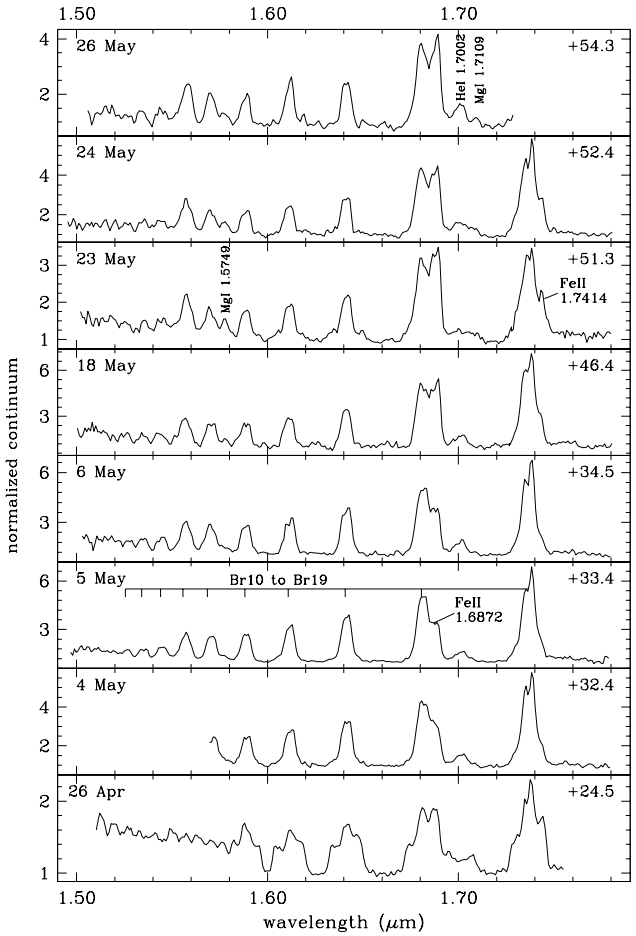

Figure 10. The H band spectra of V5588 Sgr. All spectra are normalized to unity at 1.65 μm at which the corresponding observed fluxes are (in chronological order) 9.75, 3.7, 3.47, 3.26, 2.0, 3.8, 3.29, 2.81, 2.43×10^{-17} W/cm^2/μm.

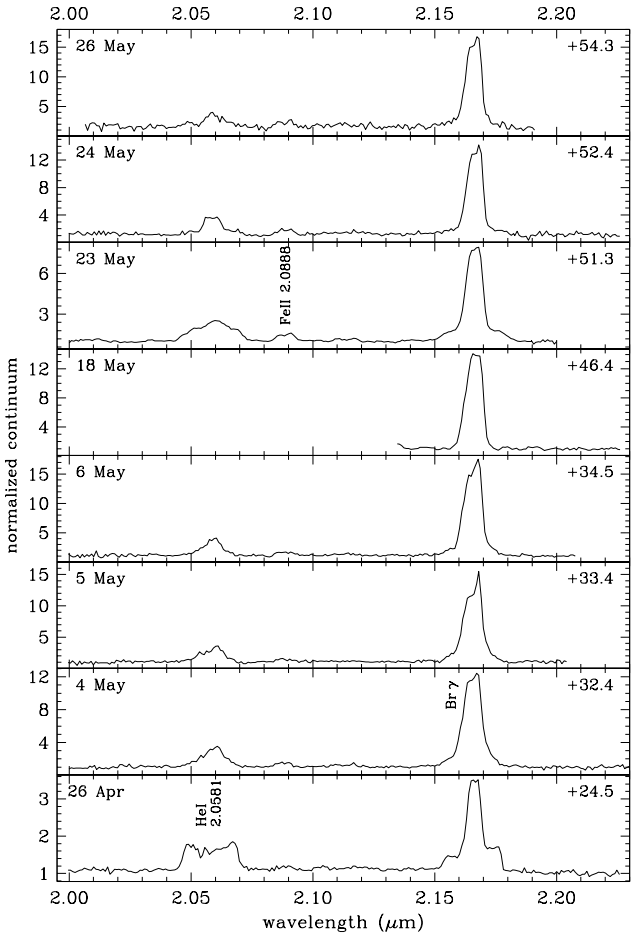

Figure 11. K band spectra of V5588 Sgr with prominent lines marked. All spectra are normalized to unity at 2.2 μm at which the corresponding observed fluxes are (in chronological order) 6.7, 2.8, 2.71, 2.64, 1.45, 2.62, 2.41, 2.2, 2.02×10^{-17} W/cm^2/μm.

6 DISCUSSION

Given the wide range of intriguing and unique features presented by V5588 Sgr, it was unfortunate that the nova was so distant and suffered extinction to such an extent that it was rather faint at maximum. This inhibited raising widespread attention among observers and thereby allowing larger telescopes to provide higher resolution and more abundant spectral observations.

The most fascinating aspect of V5588 Sgr is undoubtedly the repeated presence of nearly identical secondary maxima. The body of evidence presented in this paper suggests that they resulted from ejection at high velocity of a limited amount of material. The rise toward SdM maximum corresponds to the initial expansion in optically thick conditions, the maximum brightness to the maximum projected area reached by the expanding pseudo-photosphere, and the decline by the material turning optically thin and dissolving into surrounding space.

The extremely fast evolution of the SdM argues in favor of a limited amount of material being ejected during such episodes, with the rise to maximum taking generally less than one day and only a few days to complete the decline. It may also be argued that the ejection was in the form of a thin and almost empty shell. In fact, while its optically thick pseudo-photosphere attained a maximum a brightness in excess of that of the primary nova ejecta, as soon as it turned optically thin, its continuum emission dropped like a stone and the only emission line feature detectable was in the form of the weak pedestal, briefly seen in Hydrogen and HeI lines.

It seems that the high velocity material ejected during SdM did not collide significantly with the pre-existing slow velocity normal nova ejecta. There are no obvious traces of shocked or decelerating gas in the optical and near-IR spectra. In addition, the Swift X-ray satellite observed V5588 Sgr seven times between 30 August 2011 (while the nova was on the rise toward its sixth SdM) and 24 July 2012. The nova was only detected during the 2011 observations, at a very low average count rate of of 0.010 +/- 0.002 c/s, in contrast with the expectations from high velocity SdM material slamming onto the normal nova ejecta. Therefore, the material ejected during SdM either expanded and dissolved into the cavity left over by expanding normal ejecta or moved along spatial directions away from spatially confined main ejecta (for ex. with the normal ejecta expanding on the plane of the sky in a bipolar shape, and the high

velocity SdM material arranged orthogonal to this like in an equatorial ring or a spherical central blob).

Only the latest theoretical models of thermonuclear runaways on novae (e.g. Hillmann et al. 2014) are able to produce the type of secondary maxima seen in V5588 Sgr. Their niche in the parameter space will need further exploration, and the extensive and accurate observational data here provided for V5588 Sgr will surely help in fine tuning the models. External sources not usually accounted for by models on thermonuclear runaways on white dwarfs may also play a role, like for example the donor star being able to refuel the WD with short and repeated pulses of mass transfer. Whatever the reason was, it is striking that the energy release during SdM (at least the energy radiated through the optical bands, cf. Figure 6) declined following an exponential pattern, while at the same time the breath of the SdM was increasing as it was the time interval between two successive ones, a pattern suggesting a relaxation mechanism. In the case of the donor star refueling the WD with pulses of mass transfer, the exponential decline in energy radiated by SdM suggests that the amount of transferred mass followed a similar decline. Such mass transfer episodes does not seem being triggered by orbital geometry (like passages at periastron in a highly eccentric and long period orbit), because of the monotone increase in time separation between them poorly compares with the regularity of orbital revolutions.

The EVLA radio observations summarized by Krauss et al. (2011c) and the comparison with V4745 Sgr (Nova 2003 N.1), the only other known nova with a lightcurve resembling V5588 Sgr, does not point to an easy solution. In fact, V5588 Sgr was found to be radio quiet just before SdM N.2 and radio loud just before SdM N. 3 and 4, and it was radio quiet during SdM N.5 and immediately after the end of SdM N.2 and N.3. As noted by Krauss et al. (2011c) such rapid and repeated on-off switch in radio emission cannot be easily understood in the conventional modeling for radio emission of nova ejecta. Both V5588 Sgr and V4745 Sgr displayed several SdM, over a similar time interval and of similar brightness. However, V4745 Sgr begun as a FeII nova and did not developed a He/N spectrum at later times, e.g. it was not an hybrid nova, and its emission lines were twice as wide as in V5588 Sgr. In addition, while the spectra of V5588 Sgr did not change during SdM other than for the appearance of the weak broad pedestal, the emission lines of V4745 Sgr during SdM switched back to strong P-Cyg absorption profiles as for the primary maximum (Csák et al. 2005, Tanaka et al. 2011).

A dedicated comparison of detailed properties of the few novae that displayed one or more SdM is well beyond the scope of this paper, but surely worth considering. While information like orbital period and orbital inclination or presence of WD modulation (suggesting a significant magnetic field) are available for some of these novae, the same will be hardly achievable for V5588 Sgr given its faint magnitude in quiescence (V>21 mag), requiring the largest available telescopes for the attempt.

7 ACKNOWLEDGEMENTS

We would like to thank E. Tamajo, P. Valisa and P. Ochner for assistance with some of the spectroscopic observations. The research work at the Physical Research Laboratory is funded by the Department of Space, Government of India.

REFERENCES

Arai A., Nagashima M., Kajikawa T., and Naka C., 2011, IAUC 9203
Banerjee D.P.K. & Ashok, N.M., 2002,A&A, 395, 161
Banerjee D.P.K. & Ashok, N.M., 2012, BASI, 40, 243
Banerjee D.P.K., Das R.K., Ashok N.M., MNRAS, 2009, 399, 357
Banerjee D.P.K. & Ashok N.M., 2011, Astronomers Telegram, 3345
Bautista M. A., Rudy R. J., Venturini C. C., 2004, ApJ, 604, L129
Buscombe W., de Vaucouleurs G., 1955, Obs, 75, 170
Capaccioli M., della Valle M., Rosino L., D'Onofrio M., 1989, AJ, 97, 1622
Csák B., Kiss L. L., Retter A., Jacob A., Kaspi S., 2005, A&A, 429, 599
Das R.K., Banerjee D.P.K., Ashok N.M.,Chesneau O., 2008, MNRAS, 391, 1874
Das R.K., Banerjee D.P.K., Ashok N.M., 2009, MNRAS, 398, 375
Downes R. A., Duerbeck H. W., 2000, AJ, 120, 2007
Ferland G. J., 2003, ARA&A, 41, 517
Fiorucci M., Munari U., 2003, A&A, 401, 781
Harman D. J. et al., 2009, ASPC, 401, 246, (astro-ph 0809.4592)
Hounsell R., et al., 2010, ApJ, 724, 480
Iijima T., 2009, A&A, 505, 287
Kiyota S., 2011, IAUC, 9203, 1
Krauss M. I., et al., 2011a, ATel, 3319
Krauss M. I., et al., 2011b, ATel, 3397
Krauss M. I., et al., 2011c, ATel, 3539
Krautter J., 2008, ASPC, 401, 139
Landolt A. U., 2009, AJ, 137, 4186
Lynch D.K., Rossano G.S., Rudy R.J., Puetter R.C, 1995, AJ, 110, 2274
Lynch D. K., Wilson J. C., Rudy R. J., Venturini C., Mazuk S., Miller N.A., Puetter R. C., 2004, AJ, 127, 1089
McLaughlin D. B., 1960, in Stellar Atmospheres. J. L. Greenstein ed., University of Chicago Press, 585
Maehara H., 2011, IAUC, 9203, 1
Munari U., et al., 2008a, A&A, 492, 145
Munari U., Henden A., Valentini M., Siviero A., Dallaporta S., Ochner P., Tomasoni S., 2008, MNRAS, 387, 344
Munari U., Henden A., Valisa P., Dallaporta S., Righetti G. L., 2010, PASP, 122, 898
Munari U., et al. 2011a, CBET 2707
Munari U., Ashok N. M., Banerjee D. P. K., Righetti G. L., Dallaporta S., Cetrulo G., Englaro A., 2011b, CBET 2723
Munari U., Siviero A., Dallaporta S., Cherini G., Valisa P., Tomasella L., 2011c, NewA, 16, 209
Munari U., et al., 2012, BaltA, 21, 13
Munari U., Moretti S., 2012, BaltA, 21, 22
Munari U., 2012, JAVSO, 40, 582
Munari U., Valisa P., 2014, in Observing Techniques, Instrumentation and Science for Metre-Class Telescopes, T. Pribulla ed., CoSka, 43, 174

Naik S., Banerjee D. P. K., Ashok N. M., Das, R.K., 2010, MNRAS, 404, 367
Nishiyama K., Kabashima F., 2011, IAUC, 9203, 1
Pejcha, O. 2009, ApJ, 701, L119
Raj A., Ashok N. M., Banerjee D. P. K., 2011, MNRAS, 415, 3455
Rudy R. J., Puetter R. C., Mazuk S., Hamann, F., 2000, ApJ, 539, 166
Rudy R. J., Lynch D. K., Mazuk S., Venturini C. C., Puetter R. C., Perry R. B., 2002, BAAS, 34, 1162
Rudy R. J., Venturini C., Lynch D. K., Mazuk S., Puetter R. C., 2002, ApJ, 573, 794
Rudy R. J., Dimpel W. L., Lynch D. K., Mazuk S., Venturini C. C., Wilson J. C., Puetter R. C., Perry R. B., 2003, ApJ, 596, 1229
R. J. Rudy, R. W. Russell, M. Sitko, 2011, IAUC 9211
Seaquist, E. R., & Bode, M. F. 2008, in Cambridge Astrophys. Ser. 43, Classical Novae, eds., M. F. Bode & A. Evans, (2nd ed., Cambridge: Cambridge Univ. Press), 141
Strope R. J., Schaefer B. E., Henden A. A., 2010, AJ, 140, 34
Tanaka J., Nogami D., Fujii M., Ayani K., Kato T., 2011, PASJ, 63, 159
van den Bergh S., Younger P. F., 1987, A&AS, 70, 125
Venturini, C. C., Rudy, R. J., Lynch, D. K.,Mazuk, S., Puetter, R. C., et al. 2004, AJ, 128, 405
Wagner R. M., Depoy D. L., 1996, ApJ, 467, 860
Wallerstein G., Garnavich P. M., 1986, PASP, 98, 875
Williams R.E., 1992, AJ, 104, 725

sec.max. N.	1	2	3	4	5	6
$\mathrm{HJD}_{\mathrm{max}}$	658.5	676.5	703.5	731.8:	764.4	806.2
UT (2011)	Apr	Apr	May	Jun	Jul	Sep
	7.0	25.0	22.0	19.3:	21.9	1.7
Δt (days)		18	27	28	33	42
FWHM (days)	2.1	2.0	3.8	7.6	8.4	8.6
V peak	11.30	11.70	12.23	13.00:	14.37	14.70
ΔV	1.39	2.12	2.41	2.13:	1.42	1.54
M_V	-7.89	-7.69	-7.21	-6.42:	-4.85	-4.56
$\mathrm{Flux}_{bol}^{BVRI}$	21.2	13.6	8.9	6.7:	5.0	3.4